

Metal-insulator transition of ferromagnetic ordered double perovskites: $(\text{Sr}_{1-y}\text{Ca}_y)_2\text{FeReO}_6$ H. Kato,¹ T. Okuda,¹ Y. Okimoto,¹ Y. Tomioka,¹ K. Oikawa,² T. Kamiyama,² and Y. Tokura^{1,3,4}¹*Joint Research Center for Atom Technology (JRCAT), Tsukuba 305-0046, Japan*²*Institute of Materials Structure Science, KEK, Tsukuba 305-0801, Japan*³*Correlated Electron Research Center (CERC), National Institute of Advanced Industrial Science and Technology (AIST), Tsukuba 305-8562, Japan*⁴*Department of Applied Physics, University of Tokyo, Tokyo 113-8656, Japan*

(Received 26 November 2001; published 15 March 2002)

Temperature- and composition-control metal-insulator (M-I) transitions have been investigated for ordered double perovskites, $(\text{Sr}_{1-y}\text{Ca}_y)_2\text{FeReO}_6$. $\text{Ca}_2\text{FeReO}_6$ ($y=1$) shows the thermally induced M-I transition associated with the lattice-structural transition around 150 K. The alloyed system undergoes the M-I transition in the almost fully spin-polarized ground state around $y=0.4$ with minimal enhancement of the electronic specific-heat coefficient but with a large energy-scale (~ 1 eV) change of the optical conductivity spectrum. These results indicate the importance of electron correlation, in particular the orbital correlation of Re t_{2g} electrons, for the ferromagnetic M-I transition.

DOI: 10.1103/PhysRevB.65.144404

PACS number(s): 71.30.+h, 75.40.-s

I. INTRODUCTION

In ordered double perovskites denoted as $A_2B'B''O_6$ (A being an alkaline-earth or rare-earth ion), the transition-metal sites (perovskite B sites) are occupied alternately by different cations B' and B'' . Among them, $A_2\text{FeMO}_6$ ($A = \text{Ca}, \text{Sr}, \text{Ba}$; $M = \text{Mo}, \text{Re}$) are known to form conducting ferromagnets, in which Fe^{3+} ($3d^5, S=5/2$) and Mo^{5+} ($4d^1, S=1/2$) [or Re^{5+} ($5d^2, S=1$)] couple antiferromagnetically. Pioneering studies of these materials were done in the 1960s.¹⁻³ More lately, it was shown by the first-principles band calculation^{4,5} that the conduction band around the Fermi energy in $\text{Sr}_2\text{FeMoO}_6$ ($\text{Sr}_2\text{FeReO}_6$) is occupied solely by the $\text{Mo}^{5+} 4d$ ($\text{Re}^{5+} 5d$) t_{2g} down-spin electrons hybridized with the $\text{Fe}^{3+} 3d$ t_{2g} down-spin state, leading to a half-metallic (single-spin) character. It has also been demonstrated⁴⁻⁶ that the polycrystalline ceramics of these oxides show a large, low-field magnetoresistance even at room temperature that can be ascribed to the tunneling-type magnetoresistance occurring at the grain boundaries. The phenomena must reflect the high-spin polarization of conduction electrons characteristic of the half-metal as well as the inherently high magnetic transition temperature (T_c) in the range of 400–450 K.^{1,2} Thus, the family of half-metallic double perovskites has been attracting growing interest also in light of potential spin-electronic materials.

Among this family, $\text{Ba}_2\text{FeReO}_6$,³ $\text{Ba}_2\text{FeMoO}_6$,⁷ and $\text{Ca}_2\text{FeMoO}_6$ (Ref. 8) show ferromagnetic and metallic characteristics as do $\text{Sr}_2\text{FeMoO}_6$ and $\text{Sr}_2\text{FeReO}_6$. On the other hand, $\text{Ca}_2\text{FeReO}_6$ is rather unique: it has been known to be a ferromagnetic but also an insulating oxide with very high $T_c=538$ K.⁹ The crystal symmetry is known as monoclinic,¹⁰ which does not differ from that of metallic $\text{Ca}_2\text{FeMoO}_6$.⁸ The Fe-O-Mo and Fe-O-Re angles in those Ca-based compounds with a relatively small tolerance factor are also comparable, about 152° and 156° , respectively,^{8,10} although the respective angles are appreciably smaller than in the Sr-based analogs, $\text{Sr}_2\text{FeMoO}_6$ and $\text{Sr}_2\text{FeReO}_6$, with a

nearly straight Fe-O-Mo(Re) bond. It is well known for perovskites of transition-metal oxides¹¹ that such a bond-angle distortion reduces the effective d -electron hopping (super-transfer) energy or the one-electron bandwidth via the reduced hybridization between transition-metal d and oxygen p states. In fact, the variation of the bond angle with the change of A -site ionic size occasionally causes drastic electronic changes,¹¹ such as the bandwidth-control Mott transition and the colossal magnetoresistance. Thus, the lattice effect induced by Ca substitution as well as the change in electronic configuration between Mo and Re appears to be responsible for the metal-insulator (M-I) phenomena in the family of the ordered double perovskites.

In this paper, we investigate magnetic, electronic, thermal, and structural properties for the A -site solid solutions of ordered double perovskites, $(\text{Sr}_{1-y}\text{Ca}_y)_2\text{FeReO}_6$, to reveal composition-controlled as well as thermally induced M-I transitions. The M-I transition at the ground state may occur via the change of the bandwidth, while keeping the full spin polarization of the conduction electrons; that is, from a half-metal to a ferromagnetic (or ferrimagnetic) insulator with full moment, where the orbital degree of freedom should play an important role in the M-I transition as the only relevant degree of freedom.¹² This class of the M-I transition is intriguing, though, to our best knowledge, it has never been investigated in detail, also from the viewpoint of spin-electronic functionality.

II. EXPERIMENT

Polycrystalline samples of $(\text{Sr}_{1-y}\text{Ca}_y)_2\text{FeReO}_6$ ($0 \leq y \leq 1$) were prepared by solid-state reaction. The mixture of SrO, CaO, Fe_2O_3 , Re_2O_7 , and Re was weighted to a prescribed molar ratio and fired at 1173 K for 3 h in evacuated sealed silica tubes. Then, the samples were pelletized, and sintered at 1373 K for 3 h in evacuated sealed silica tubes. The composition of synthesized polycrystals was confirmed to be stoichiometric (Sr:Ca:Fe:Re = $2-2y:2y:1:1$) by induction coupled plasma spectroscopy analysis. The crystal

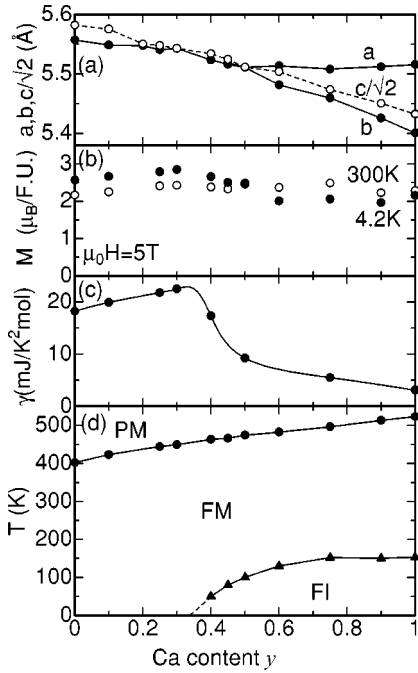


FIG. 1. The y dependence of (a) lattice constants, (b) magnetization (M) at a field of 5 T, (c) the electronic specific-heat coefficient γ , and (d) the electronic phase diagram of $(\text{Sr}_{1-y}\text{Ca}_y)_2\text{FeReO}_6$. PM, FM, and FI in (c) stands for paramagnetic metal, ferromagnetic metal, and ferromagnetic (or ferrimagnetic) insulator, respectively. Solid lines and dashed lines are merely guides to the eyes.

structure was checked by powder x-ray diffraction. The crystal symmetry at room temperature was tetragonal $I4/mmm$ ($y < 0.5$) and orthorhombic $Pmm2$ ($y > 0.5$). Figure 1(a) shows the lattice constants of $(\text{Sr}_{1-y}\text{Ca}_y)_2\text{FeReO}_6$. At $0.3 < y < 0.5$, the length of $c_0/\sqrt{2}$ is almost the same as that of a_0 , indicating nearly cubic symmetry. The Rietveld refinement also indicated that the degree of ordering of Fe and Re on the B sites was more than 95% in all the samples. As for the end ($y=1$) compound $\text{Ca}_2\text{FeReO}_6$, neutron powder-diffraction data were also collected at various temperatures to obtain the precise structural properties.¹³

Magnetization was measured with a commercial superconducting quantum interference device magnetometer. The ac susceptibility up to 550 K was also measured to evaluate the ferromagnetic transition temperature T_c by a resistance bridge. Resistivity was measured with a standard dc four-probe technique. The specific heat was measured by the relaxation method down to 0.5 K. We measured reflectivity spectra $[R(\omega)]$ for $(\text{Sr}_{1-y}\text{Ca}_y)_2\text{FeReO}_6$. $R(\omega)$ spectra were measured using a Fourier-transform-type interferometer for 0.01–0.8 eV and a grating-type monochromator for 0.6–36 eV. For the measurement above 5 eV, we made use of synchrotron radiation at the Ultraviolet Synchrotron Orbital Radiation Facility, Institute for Molecular Science. The temperature (T) dependence of the spectra was measured from 0.01 to 3.0 eV and extrapolated by the room-temperature data above 3 eV. The optical conductivity spectra $[\sigma(\omega)]$ were obtained by a Kramers-Kronig analysis of $R(\omega)$.

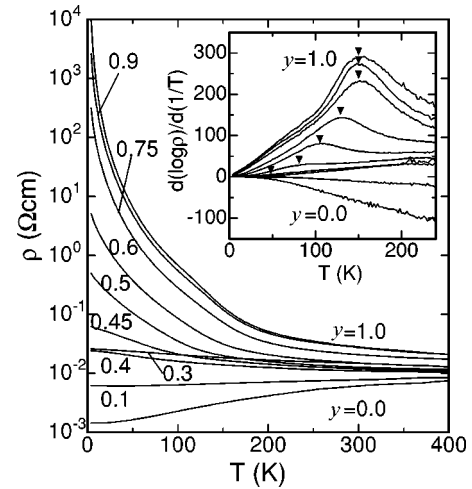


FIG. 2. The temperature (T) profiles of resistivity (ρ) of $(\text{Sr}_{1-y}\text{Ca}_y)_2\text{FeReO}_6$ ($0 \leq y \leq 1$). The inset shows the T dependence of $d(\log_{10}\rho)/d(1/T)$.

III. RESULTS AND DISCUSSION

A. Phase diagram of $(\text{Sr}_{1-y}\text{Ca}_y)_2\text{FeReO}_6$

Figure 2 shows the T dependence of resistivity (ρ) for $(\text{Sr}_{1-y}\text{Ca}_y)_2\text{FeReO}_6$. While ρ is about 10^{-2} Ωcm at room temperature for all the samples, the Ca content (y) affects the T dependence of ρ dramatically. For $y \leq 0.3$ the compounds show a metallic or semimetallic behavior down to the lowest temperature. For $y \geq 0.4$, ρ increases with decreasing temperature below 150 K. The variation of the T dependence of ρ with y is more clearly discerned in $d(\log_{10}\rho)/d(1/T)$ - T curves as shown in the inset to Fig. 2. For $y \leq 0.3$ the curves show no anomaly, but for $y \geq 0.4$ they have peaks at 100–150 K, indicating an electronic change around this peak temperature (T^*).

Figure 1(d) shows the electronic phase diagram of $(\text{Sr}_{1-y}\text{Ca}_y)_2\text{FeReO}_6$. Although $d\rho/dT < 0$, we assigned the high- T phase above T^* as metallic, based on the relatively high conductivity as well as the spectral shape of $\sigma(\omega)$ that is not gapped (see below). The observed T_c increases monotonically from 400 K to 525 K with increasing y . At room temperature, all the samples are in a ferromagnetic metallic state, while the ferromagnetic insulating state emerges for $y \geq 0.4$ below 150 K. The M-I transition temperature is tentatively defined as the peak temperature of the $d(\log_{10}\rho)/d(1/T)$ - T curve that coincides with the structural transition temperature in the case of $y=1$, as shown later. At the compositional phase boundary around $y=0.4$ between the ferromagnetic metallic and the ferromagnetic insulating phases, the coercive force at low temperatures increases and the saturation magnetization decreases, also implying a change in the electronic state. However, the ground-state magnetization is 2.0–2.8 $\mu_B/\text{f.u.}$, indicating the almost full spin polarization or moment irrespective of y at the ground state [Fig. 1(b)].

B. Specific heat

The low-temperature specific heat (C) was measured to evaluate the electronic specific-heat coefficient (γ).

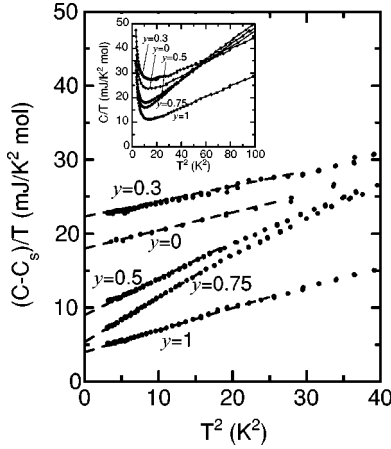


FIG. 3. The low-temperature specific heat of $(\text{Sr}_{1-y}\text{Ca}_y)_2\text{FeReO}_6$ ($0 \leq y \leq 1$) plotted as $(C - C_s)/T$ versus T^2 . Here, C_s stands for the Schottky component caused by the Re nuclear moments. The inset shows the raw data of specific heat plotted as C/T versus T^2 . Dashed lines are merely guides to the eyes.

Figure 3 shows the low-temperature specific heat of $(\text{Sr}_{1-y}\text{Ca}_y)_2\text{FeReO}_6$ plotted as $(C - C_s)/T$ versus T^2 . As shown in the inset, the Schottky components (C_s) caused by the Re nuclear moments are dominant at low temperatures (< 3 K) in all the compounds that are proportional to $1/T^2$. Coefficients of the $1/T^2$ term are 0.122–0.155 JK/mol, in accord with that reported for $\text{Ca}_2\text{FeReO}_6$ ($y = 1$) in a previous work.⁹ The value linearly increases with the increase of y , indicating the increase of inner field applied on Re atoms. The γ values were evaluated from the $(C - C_s)/T$ values extrapolated to 0 K at 0 T, because a magnetic field of 6 T was confirmed not to affect the low-temperature specific heat significantly.^{14,15} The obtained electronic specific-heat coefficient (γ) is shown in Fig. 1(c). The γ value for $y = 0$ is about 18 mJ/K²mol, and the density of state at the Fermi level, $N(E_F)$, is estimated to be 4.6×10^{24} (eV⁻¹ mol⁻¹) by using the relation that $\gamma = 1/3 \pi^2 k_B^2 N(E_F)$, which is twice as large as the local-density approximation calculation result [2.1×10^{24} (eV⁻¹ mol⁻¹)].⁵ As the M-I phase boundary is approached with the increase of y , the γ value slightly increases and becomes about 22 mJ/K²mol around $y = 0.3$. With the increase of y above 0.4, the γ value steeply decreases in accord with the M-I transition, signaling the sudden shrink of the Fermi surface perhaps due to the correlation of the Re t_{2g} orbital as discussed below. Such a behavior is similar to that observed in the filling-control M-I transition in the low-doped region of half-metallic manganites,¹⁵ although γ in the insulating ground state remains finite in the present compound. The increase of the γ value implies the mass-renormalization effect as observed in the vicinity of the Mott transition,¹¹ but the absence of remarkable enhancement may come from the absence of the spin fluctuation due to the nearly full spin polarization.¹⁵

C. Optical conductivity

To clarify the electronic-structural change upon the M-I transition for $(\text{Sr}_{1-y}\text{Ca}_y)_2\text{FeReO}_6$, the T and y dependencies

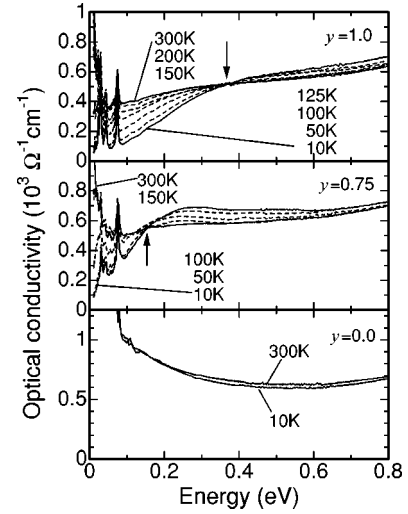


FIG. 4. Optical conductivity spectra of $(\text{Sr}_{1-y}\text{Ca}_y)_2\text{FeReO}_6$ at various temperatures (10–300 K) for $y = 0.0, 0.75,$ and 1.0 .

of the optical conductivity spectrum $\sigma(\omega)$ have been investigated. Figure 4 shows the T dependence of $\sigma(\omega)$ for $y = 0, 0.75,$ and 1 . The spectra are not gapped and contain Drude components below 0.1 eV above 150 K. For $y = 0$, $\sigma(\omega)$ above 0.1 eV scarcely changes with the decrease of T down to 10 K. For $y = 0.75$ and 1 , by contrast, the Drude component disappears and the gap structure appears below 150 K, indicating the occurrence of the M-I transition with the variation of the temperature. The gap formation with the decrease of T accompanies the appreciable change of the optical conductivity spectrum over 1 eV. The spectral weight is transferred from low to high energy through the isosbestic (equal-absorption) point as indicated by vertical arrows in Fig. 4. Such a large-energy-scale change in the course of the M-I transition is characteristic of the Mott transition in the strongly correlated electron system, ensuring that the present half-metallic oxide is also on the verge of the Mott transition.¹⁶ The isosbestic point is observed to gradually decrease with the decrease of y , 0.37 eV and 0.16 eV for $y = 1$ and 0.75 , respectively. This suggests that the optical gap gradually disappears with the decrease of y toward the ground-state M-I transition point ($y \approx 0.4$).

D. T dependence of charge dynamics in $\text{Ca}_2\text{FeReO}_6$

We summarize in Fig. 5 the T dependence of [Fig. 5(a)] lattice constants, [Fig. 5(b)] spectral-weight loss during the gap formation, [Fig. 5(c)] magnetization, and [Fig. 5(d)] resistivity for $\text{Ca}_2\text{FeReO}_6$ ($y = 1$) that shows the typical M-I transition with the variation of T . The low-energy spectral weight of $\sigma(\omega)$ [Fig. 4, upper], that measures the kinetic energy of conduction electrons, is transferred to the high-energy side above the isosbestic point in the course of the M-I transition. To estimate the transferred weight, we have calculated the effective number of electrons (N_{eff}), which is defined as

$$N_{\text{eff}}(\omega) = \frac{m_0}{\pi e^2 N} \int_0^{\omega_c} \sigma(\omega) d\omega.$$

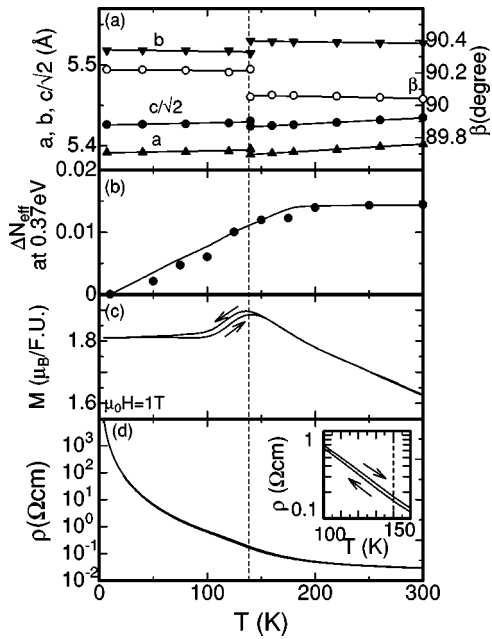


FIG. 5. The temperature (T) dependence of (a) lattice constants, (b) spectral-weight change below 0.37 eV (ΔN_{eff}) due to the charge-gap formation, (c) magnetization (M) at a field of 1 T, and (d) resistivity (ρ) for $\text{Ca}_2\text{FeReO}_6$. The inset in (d) shows a magnification of the ρ - T curve at 100–150 K, in which resistivity shows a hysteresis. Solid lines in (a) and (b) are merely guides to the eyes.

Here, m_0 is the free-electron mass and N the number of B -site ion pairs (Fe and Re) per unit volume. The cutoff energy ($\hbar\omega_c$) adopted for the estimate is the isosbestic point, 0.37 eV. The transferred spectral weight ΔN_{eff} in the course of the M-I transition is represented as $\Delta N_{\text{eff}}(T) = N_{\text{eff}}(T) - N_{\text{eff}}(T = 10 \text{ K})$. Lattice constants were obtained by Rietveld analysis of neutron powder diffraction. As shown in Fig. 5(a), β changes from 90° to 90.2° at 140 K, indicating that the transition from orthorhombic to monoclinic structure takes place. The monoclinic phase is not observed at 160 K, while the nearly orthorhombic phase disappears below 120 K. This means that two phases coexist only in the temperature range of 120–160 K, typical of the first-order transition in the presence of some disorder. The N_{eff} also starts to decrease at 140 K, corresponding to the peak temperature in the $d(\log_{10}\rho)/d(1/T)$ plot. In the corresponding temperature region, thermal hysteresis is observed for magnetization and resistivity, which also reflects the first-order nature of the M-I transition in $\text{Ca}_2\text{FeReO}_6$.

It is worth noting that in spite of the existence of the clear optical gap the γ value (T -linear component in specific heat) remains finite even in $\text{Ca}_2\text{FeReO}_6$. Note that this cannot be

ascribed to the coexistence of the metallic and insulating phases at low temperature, as is evident from the aforementioned neutron-diffraction study on the lattice-structural change. According to the Mössbauer measurements,¹⁰ the valence states of Fe and Re are high-spin Fe^{3+} and Re^{5+} , respectively, and the $\text{Re}^{5+} 5d t_{2g}^2$ states are triply degenerate (or equivalently, a t_{2g} hole can have three degenerate states d_{xy} , d_{yz} , and d_{zx}), retaining the orbital degree of freedom. The correlation of the Re t_{2g} orbital is likely to cause the thermally induced M-I transition, which may be a driving force of the nearly orthorhombic to monoclinic lattice-structural transition as well. Furthermore, Re atoms form an fcc lattice in the ordered double perovskite structure. Then, the nearest-neighboring Re atoms make a tetragon, and hence the orbital ordering of $\text{Re}^{5+} t_{2g}$ electrons is likely to be frustrated. The finite γ value in the insulating phase ($y = 0.4$ – 1.0) may be interpreted as the glass state of the $\text{Re}^{5+} t_{2g}$ orbital in analogy to the conventional spin-glass state that may give rise to the residual T -linear form of specific heat in spite of the charge-gapped state as observed.

IV. SUMMARY

In summary, we have investigated the M-I phenomena in the ordered double perovskites $(\text{Sr}_{1-y}\text{Ca}_y)_2\text{FeReO}_6$ with controlled one-electron bandwidth. Throughout the composition, the compound is metallic and ferromagnetic at room temperature with high T_c of 400–525 K, but it undergoes the M-I transition with decreasing temperature for $y \geq 0.4$. The Ca substitution (y) dramatically affects the electronic structure, and the M-I transition occurs around $y = 0.4$ at the ground state while keeping the almost fully spin-polarized state. The ground-state M-I transition, that is not accompanied by appreciable mass renormalization, is likely related to the correlation of the Re t_{2g} orbital. The insulating ground state in the Ca-rich side is perhaps described as the Re t_{2g} orbital ordered state or its glass-state analog associated with the monoclinic lattice distortion.

ACKNOWLEDGMENTS

The authors would like to thank S. Miyasaka, K. Nakanishi, H. Yamada, and N. Nagaosa for enlightening discussions. This work, partly supported by NEDO (New Energy and Industrial Technology Development Organization of Japan), was performed under a joint research agreement between the National Institute of Advanced Industrial Science and Technology (AIST) and the Angstrom Technology Partnership (ATP).

¹F.K. Patterson, C.W. Moeller, and R. Word, *Inorg. Chem.* **2**, 196 (1963).

²J. Longo and R. Word, *J. Am. Chem. Soc.* **83**, 2816 (1961).

³A.W. Sleight and J.F. Weiher, *J. Phys. Chem. Solids* **33**, 679 (1972).

⁴K.-I. Kobayashi, T. Kimura, H. Sawada, K. Terakura, and Y. Tokura, *Nature (London)* **395**, 677 (1998).

⁵K.-I. Kobayashi, T. Kimura, Y. Tomioka, H. Sawada, K. Terakura, and Y. Tokura, *Phys. Rev. B* **59**, 11 159 (1999).

⁶T.H. Kim, M. Uehara, S-W. Cheong, and S. Lee, *Appl. Phys.*

- Lett. **74**, 1737 (1999).
- ⁷A. Maignan, B. Raveau, C. Martin, and M. Hervieu, *J. Solid State Chem.* **144**, 224 (1999).
- ⁸J.A. Alonso, M.T. Casais, M.J. Martinez-Lope, J.L. Martinez, P. Velasco, A. Munoz, and M.T. Fernandez-Diaz, *Chem. Mater.* **12**, 161 (2000).
- ⁹W. Prellier, V. Smolyaninova, A. Biswas, C. Galley, R.L. Greene, K. Ramesha, and J. Gopalakrishnan, *J. Phys.: Condens. Matter* **12**, 965 (2000).
- ¹⁰J. Gopalakrishnan, A. Chattopadhyay, S.B. Ogale, T. Venkatesan, R.L. Greene, A.J. Millis, K. Ramesha, B. Hannoyer, and G. Marrest, *Phys. Rev. B* **62**, 9538 (2000).
- ¹¹M. Imada, A. Fujimori, and Y. Tokura, *Rev. Mod. Phys.* **30**, 1039 (1998).
- ¹²Y. Tokura and N. Nagaosa, *Science* **288**, 462 (2000).
- ¹³T. Kamiyama, S. Torii, K. Mori, K. Oikawa, S. Itoh, M. Furusaka, S. Satoh, T. Egami, F. Izumi, and H. Asano, *Mater. Sci. Forum* **321-324**, 302 (2000).
- ¹⁴Y. Tomioka, T. Okuda, Y. Okimoto, R. Kumai, K.-I. Kobayashi, and Y. Tokura, *Phys. Rev. B* **61**, 422 (2000).
- ¹⁵T. Okuda, A. Asamitsu, Y. Tomioka, T. Kimura, Y. Taguchi, and Y. Tokura, *Phys. Rev. Lett.* **81**, 3203 (1998).
- ¹⁶Y. Okimoto, T. Katsufuji, T. Ishikawa, A. Urushibara, T. Arima, and Y. Tokura, *Phys. Rev. Lett.* **75**, 109 (1995).